Depletion of the superfluid reservoir in neutron-star crust

Nicolas Chamel

Institute of Astronomy and Astrophysics
Université Libre de Bruxelles, Belgium

Coimbra, 26 September 2018

Open question

The interior of a neutron star is thought to contain differents kinds of superfluids and superconductors in the crust and in the core.

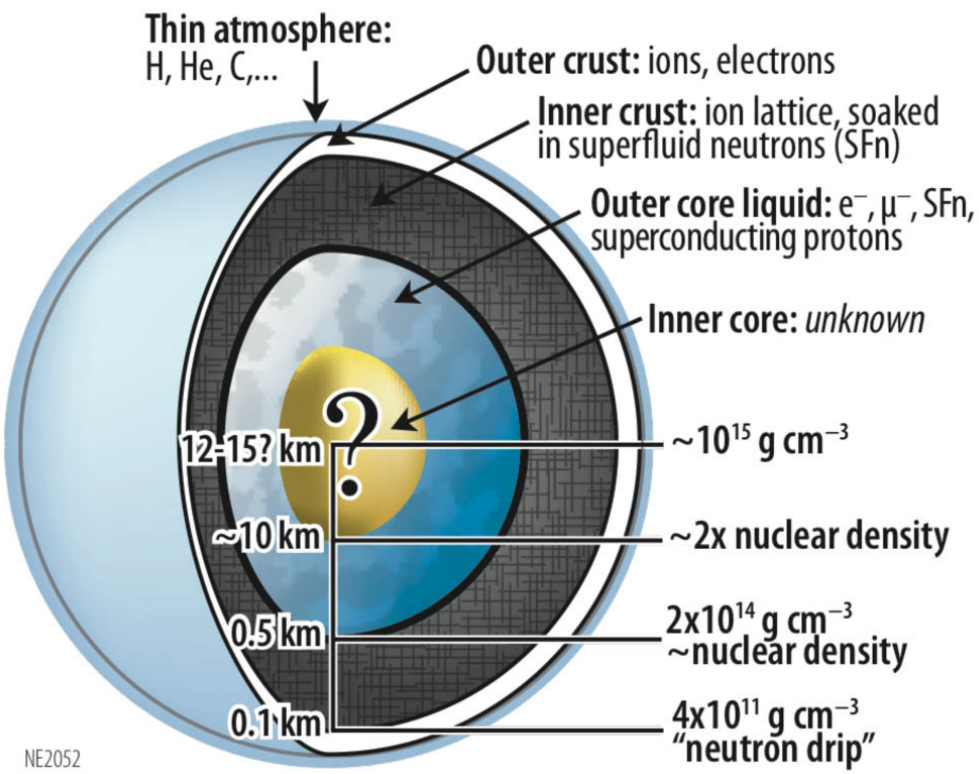

For a recent review: *Chamel, J. Astrophys. Astr. 38, 43 (2017)*

<u>Question:</u> How do superfluid neutrons flow through the crust?

Superfluidity in an inhomogeneous medium

The **breaking of translational symmetry** leads to the depletion of the superfluid reservoir, even at $T = 0$.

Leggett, Phys. Rev. Lett. 25, 1543 (1970)

Can a Solid Be "Superfluid"?

A. J. Leggett
School of Mathematical and Physical Sciences, University of Sussex, Falmer, Brighton, Sussex, England
(Received 15 September 1970)

It is suggested that the property of nonclassical rotational inertia possessed by superfluid liquid helium may be shared by some solids. In particular, nonclassical rotational inertia very probably occurs if the solid is Bose-condensed as recently proposed by Chester. Anomalous macroscopic effects are then predicted. However, the associated superfluid fraction is shown to be very small (probably $\lesssim 10^{-4}$) even at $T = 0$, so that these effects could well have been missed. Direct tests are proposed.

Examples:

- superfluid helium in porous media,
- superconducting electrons in solids,
- dilute atomic superfluids in optical lattices.

Superfluidity in neutron-star crust

Similarly, **superfluid neutrons in neutron-star crusts do not flow freely** despite the absence of viscous drag.

The neutron current in the crust rest frame can be written as

$$\boldsymbol{j_n} = n_n^s \boldsymbol{v_n}$$

$\boldsymbol{v_n}$ is the neutron "superfluid velocity" (momentum)

n_n^s is the neutron superfluid density

The neutron superfluid density n_n^s is generally smaller than the density n_n^f of free neutrons due to the **breaking of translational symmetry**.

Recent review:

Chamel, J. Low. Temp. Phys. 189, 328 (2017) - arXiv:1707.07854

Microscopic approach: density functional theory

In the **Hartree-Fock-Bogoliubov method**, neutrons are described by **independent quasiparticles in self-consistent "mean" fields**:

$$\sum_{\sigma'} \begin{pmatrix} h(\boldsymbol{r})_{\sigma\sigma'} & \Delta(\boldsymbol{r})\delta_{\sigma\sigma'} \\ \Delta(\boldsymbol{r})\delta_{\sigma\sigma'} & -h(\boldsymbol{r})_{\sigma\sigma'} \end{pmatrix} \begin{pmatrix} \Psi_1(\boldsymbol{r},\sigma') \\ \Psi_2(\boldsymbol{r},\sigma') \end{pmatrix} = E \begin{pmatrix} \Psi_1(\boldsymbol{r},\sigma) \\ \Psi_2(\boldsymbol{r},\sigma) \end{pmatrix}$$

- $h(\boldsymbol{r})_{\sigma'\sigma} \equiv -\nabla \cdot B(\boldsymbol{r})\nabla\delta_{\sigma\sigma'} + U(\boldsymbol{r})\delta_{\sigma\sigma'} - \mu\delta_{\sigma\sigma'}$ is the single-particle Hamiltonian with μ the chemical potential,
- $\Delta(\boldsymbol{r})$ is the potential describing the formation of pairs.

The HFB equations are **highly nonlinear** since $h(\boldsymbol{r})_{\sigma'\sigma}$ and $\Delta(\boldsymbol{r})$ are determined by the set of occupied wave functions $\{\Psi_1(\boldsymbol{r},\sigma); \Psi_2(\boldsymbol{r},\sigma)\}$.

The HFB method reduces to the BCS theory in homogeneous matter.

Dobaczewski & Nazarewicz, in "50 years of Nuclear BCS" (World Scientific Publishing, 2013), pp.40-60

Density functional theory in a periodic medium

Floquet-Bloch theorem

> *I found to my delight that the wave differed from the plane wave of free electrons only by a periodic modulation.*

Bloch, Physics Today 29 (1976), 23-27.

The wave functions satisfy

$$\Psi_{1\alpha\boldsymbol{k}}(\boldsymbol{r}+\boldsymbol{\ell},\sigma) = e^{\mathrm{i}\,\boldsymbol{k}\cdot\boldsymbol{\ell}}\Psi_{1\alpha\boldsymbol{k}}(\boldsymbol{r},\sigma)$$
$$\Psi_{2\alpha\boldsymbol{k}}(\boldsymbol{r}+\boldsymbol{\ell},\sigma) = e^{\mathrm{i}\,\boldsymbol{k}\cdot\boldsymbol{\ell}}\Psi_{2\alpha\boldsymbol{k}}(\boldsymbol{r},\sigma)$$

for any lattice vector $\boldsymbol{\ell}$.

- Band index α (rotational symmetry around each lattice site)
- Wave vector $\boldsymbol{k}$ (translational symmetry of the crystal).

Chamel, Goriely, Pearson, in "50 years of Nuclear BCS" (World Scientific Publishing, 2013), pp.284-296.

Multi-band BCS theory

Due to **proximity effects**, $\Delta(\boldsymbol{r})$ varies very smoothly.

The HFB equations can thus be well-approximated by the **multiband BCS gap equations**:

$$\Delta_{\alpha\boldsymbol{k}} = -\frac{1}{2}\sum_{\beta}\int \frac{\mathrm{d}^3\boldsymbol{k'}}{(2\pi)^3}\,\bar{v}^{\mathrm{pair}}_{\alpha\boldsymbol{k}\beta\boldsymbol{k'}}\,\frac{\Delta_{\beta\boldsymbol{k'}}}{E_{\beta\boldsymbol{k'}}}\tanh\frac{E_{\beta\boldsymbol{k'}}}{2k_{\mathrm{B}}T}$$

$$E_{\alpha\boldsymbol{k}} = \sqrt{(\varepsilon_{\alpha\boldsymbol{k}}-\mu)^2+\Delta^2_{\alpha\boldsymbol{k}}}$$

$$\bar{v}^{\mathrm{pair}}_{\alpha\boldsymbol{k}\beta\boldsymbol{k'}} = \int \mathrm{d}^3r\, v^{\pi}[n_n(\boldsymbol{r}), n_p(\boldsymbol{r})]\,|\varphi_{\alpha\boldsymbol{k}}(\boldsymbol{r})|^2|\varphi_{\beta\boldsymbol{k'}}(\boldsymbol{r})|^2$$

where $v^{\pi}[n_n(\boldsymbol{r}), n_p(\boldsymbol{r})]$ is an effective pairing interaction.

The wave functions $\varphi_{\alpha\boldsymbol{k}}$ and the energies $\varepsilon_{\alpha\boldsymbol{k}}$ are given by

$$-\boldsymbol{\nabla}\cdot B(\boldsymbol{r})\boldsymbol{\nabla}\varphi_{\alpha\boldsymbol{k}}(\boldsymbol{r},\sigma) + U(\boldsymbol{r})\varphi_{\alpha\boldsymbol{k}}(\boldsymbol{r},\sigma) = \varepsilon_{\alpha\boldsymbol{k}}\varphi_{\alpha\boldsymbol{k}}(\boldsymbol{r},\sigma)$$

Chamel et al., Phys.Rev.C81,045804 (2010).

Multi-band BCS superconductors

Multi-band superconductors were first studied in 1959 but clear evidence were found only in 2001 with the discovery of MgB_2.

Electrons in different bands feel different pairing interactions leading to different pairing gaps:

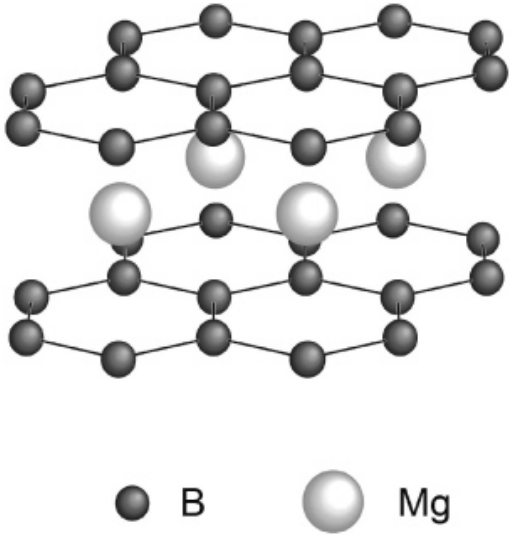

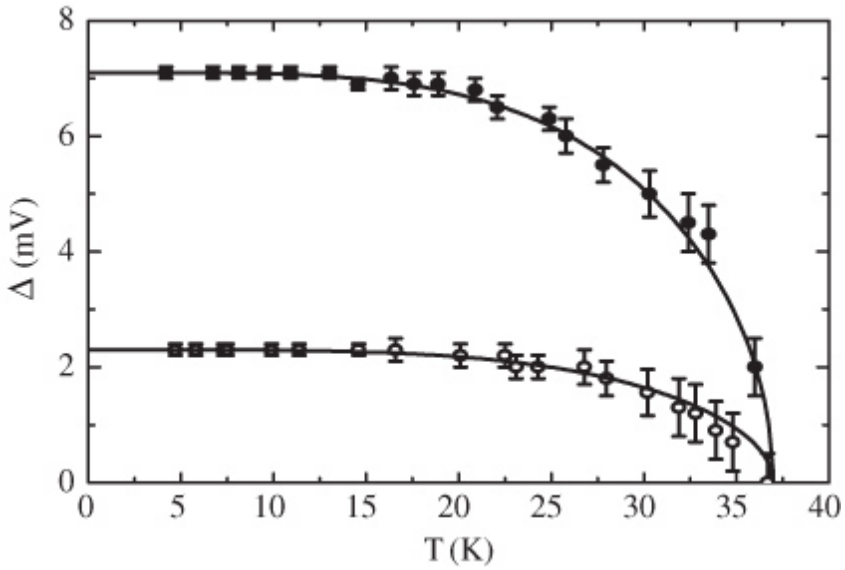

X. X. Xi, Rep. Prog. Phys.71, 116501 (2008)

Multi-band BCS neutron superfluid

In the crust of a neutron star, the number of bands is $\sim 10^2 - 10^3$!

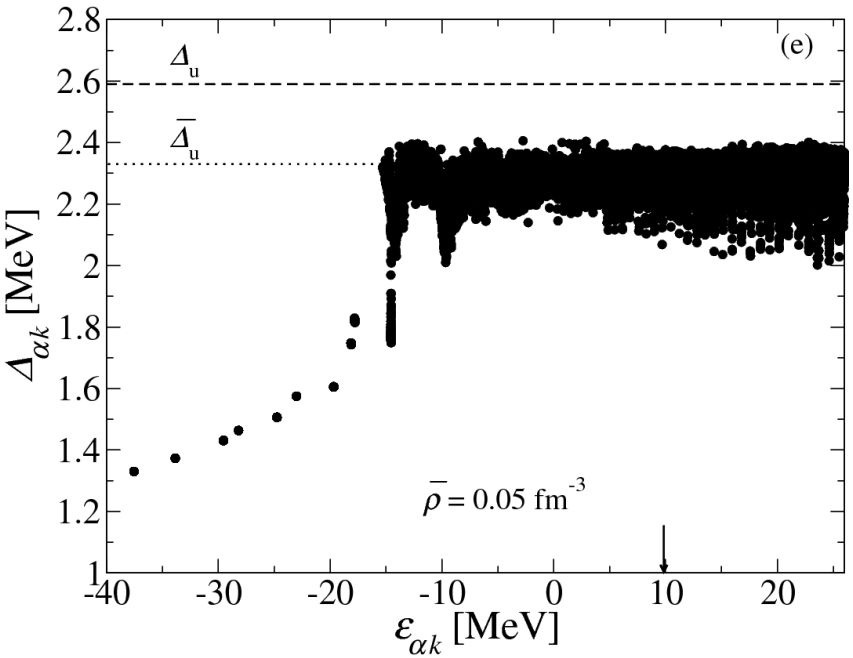

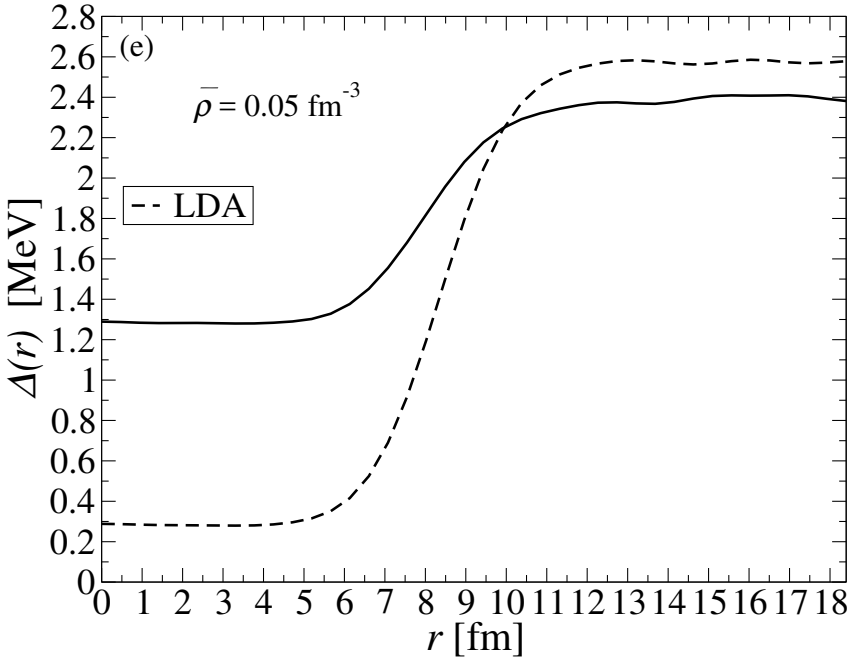

Chamel et al., Phys.Rev.C81,045804 (2010)

Superfluidity permeates clusters because Cooper pairs are loosely bound (coherence length $\gg$ cluster size).

Neutron superfluid fraction

The neutron superfluid density at $T = 0$ is given by

$$n_n^s = \frac{m_n}{24\pi^3\hbar^2} \sum_\alpha \int |\nabla_{\boldsymbol{k}} \varepsilon_{\alpha\boldsymbol{k}}|^2 \frac{\Delta_{\alpha\boldsymbol{k}}^2}{\sqrt{(\varepsilon_{\alpha\boldsymbol{k}} - \mu)^2 + \Delta_{\alpha\boldsymbol{k}}^2}^3} \mathrm{d}^3 k$$

In the **weak coupling** limit $\Delta_{\alpha\boldsymbol{k}}/\mu \to 0$, it is fully determined by the shape of the Fermi surface **independently of pairing**:

$$n_n^s \approx \frac{m_n}{24\pi^3\hbar^2} \sum_\alpha \int_{\mathrm{F}} |\nabla_{\boldsymbol{k}} \varepsilon_{\alpha\boldsymbol{k}}| \mathrm{d}\mathcal{S}^{(\alpha)}$$

Carter,Chamel,Haensel,Nucl.Phys.A748,675 (2005); Nucl.Phys.A759,441(2005)

Systematic band-structure calculations showed that the superfluid fraction $\lesssim 10\%$ at densities $\sim 0.02 - 0.04$ fm^{-3}: **most neutrons are entrained by the crust**.

Chamel,Phys.Rev.C85,035801(2012).

Band structure and Fermi surface

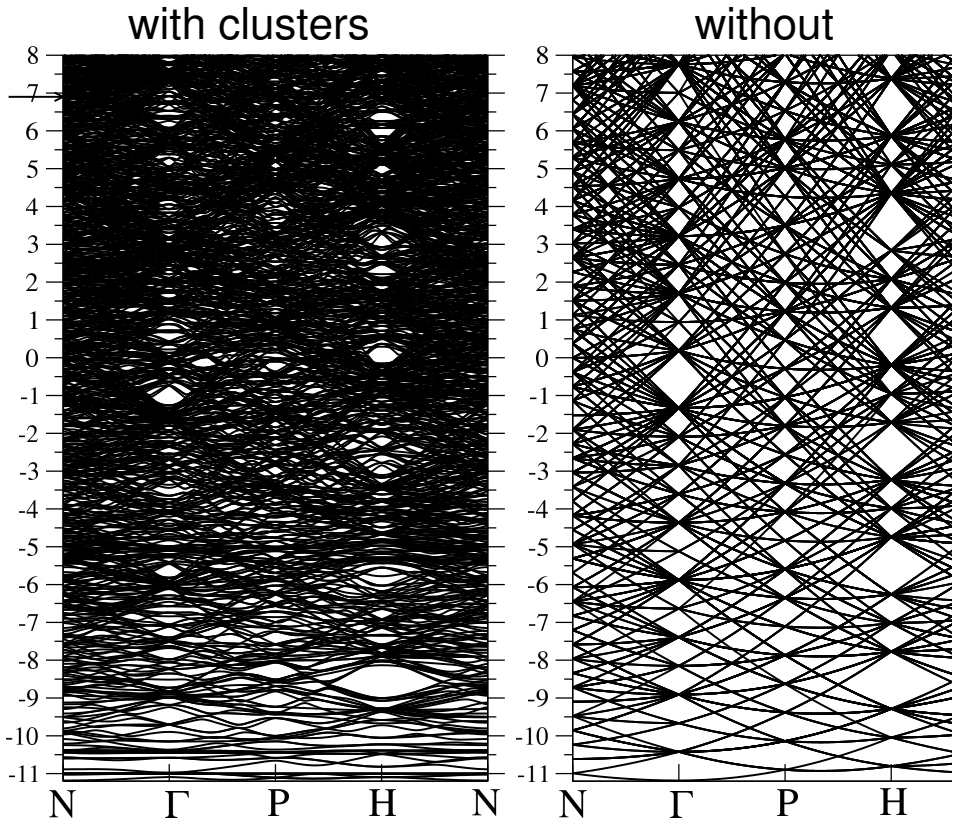

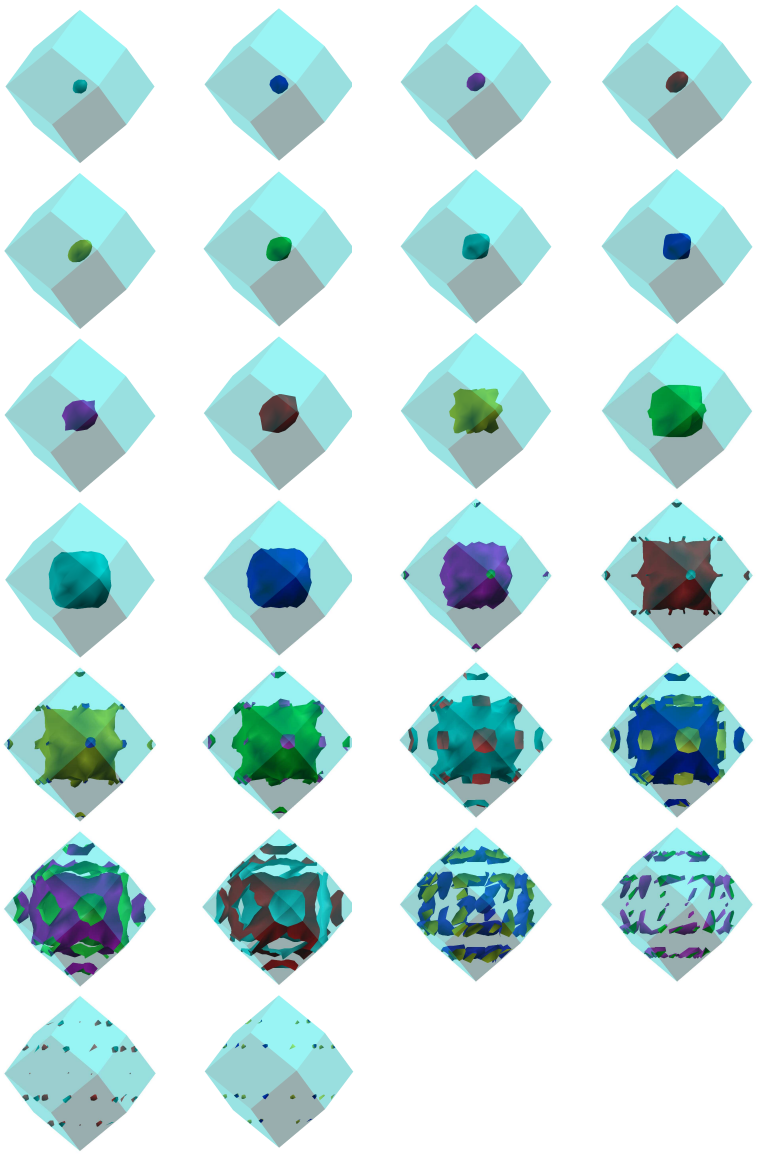

The breaking of translational symmetry leads to strong distortions of the Fermi surface.

Chamel,Phys.Rev.C85,035801(2012)

Hydrodynamic approach

The role of pairing was examined in the **strong coupling limit** using a **classical hydrodynamical** treatment.

- Superfluidity condition: $\boldsymbol{v_n} = \dfrac{\hbar}{2m_n}\nabla\phi$
- Incompressible superfluid flow: $\nabla \cdot \boldsymbol{v_n} = 0$
- Uniform spherical clusters with sharp surfaces.

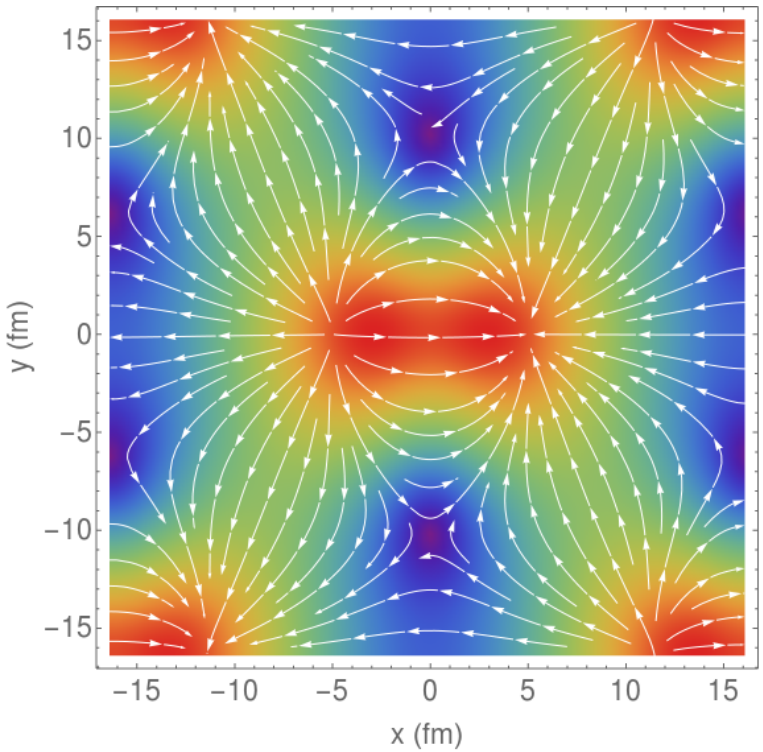

Classical potential flow $\Delta\phi = 0$.

The superfluid fraction can be extracted from the velocity field:

$$\boldsymbol{j_n} = \frac{1}{\mathcal{V}_{\text{cell}}} \int_{\text{cell}} n_n(\boldsymbol{r})\nabla\phi(\boldsymbol{r})$$

Martin&Urban,Phys.Rev.C94, 065801(2016)

Classical potential flow past obstacles

Permeability of the clusters:
$\delta = 0$ no superfluidity,
$\delta = 1$ superfluidity everywhere.
Martin&Urban,Phys.Rev.C94,065801(2016)

Added perturbations from different clusters are negligible.
Epstein, ApJ333, 880 (1988)

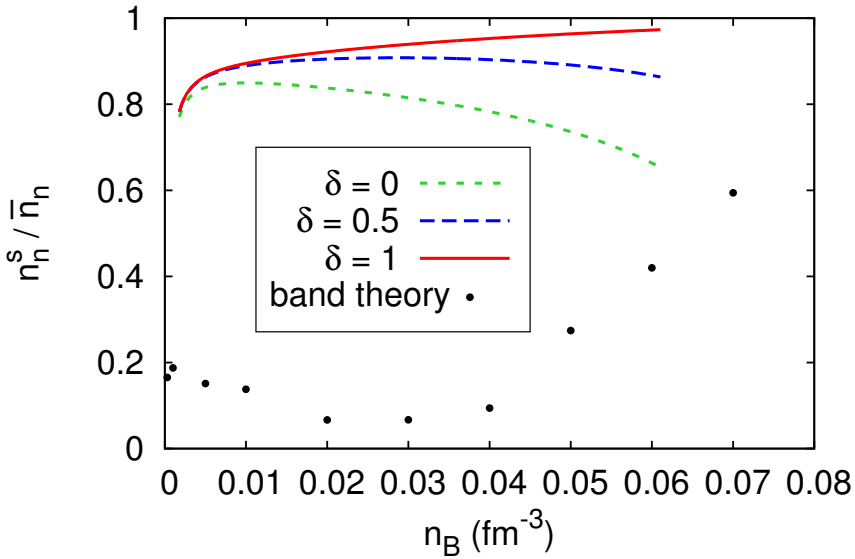

The potential flow past a single cluster can be solved analytically:

$$\frac{n_n^s}{n_n^f} = 1 + 3\frac{\mathcal{V}_{\rm cl}}{\mathcal{V}_{\rm cell}}\frac{\delta - \gamma}{\delta + 2\gamma} \Rightarrow 1 - \frac{3}{2}\frac{\mathcal{V}_{\rm cl}}{\mathcal{V}_{\rm cell}} \leq \frac{n_n^s}{n_n^f} \leq 1 + 3\frac{\mathcal{V}_{\rm cl}}{\mathcal{V}_{\rm cell}}$$

Magierski&Bulgac,Act.Phys.Pol.B35,1203(2004); Magierski, IJMPE13, 371(2004)
Sedrakian, Astrophys.Spa.Sci.236, 267(1996); Epstein, ApJ333, 880 (1988)

The superflow is found to be only **weakly perturbed** by clusters.
However, the strong coupling regime is usually not reached.

Suppression of band structure effects by pairing?

Solving the HFB equations, Watanabe&Pethick found that the flow

- is **more strongly perturbed than predicted by classical hydrodynamics at $\bar{n} = 0.03$ fm^{-3}**,
- **but much less than band calculations without pairing**.

Watanabe&Pethick,PRL119,062701(2017)

Chamel (2012)		Wanatabe&Pethick (2017)
$n_n^s/n_n \sim 8\%$		$n_n^s/n_n \sim 70\%$
HF (no pairing)	vs	HFB
3D lattice		1D lattice
self-consistent potentials		simplified potentials (cosine)
exact (analytical) formula		various approximations

$n_n^s/n_n \sim 6\%$ was obtained in 2005 from 3D band calculations (no pairing) with a different crust model.

Chamel, Nucl. Phys. A747,109 (2005)

Suppression of band structure effects by pairing?

Band-structure effects arise from the single-particle equation:

$$-\nabla \cdot B(\boldsymbol{r})\nabla\varphi_{\alpha\boldsymbol{k}}(\boldsymbol{r},\sigma) + U(\boldsymbol{r})\varphi_{\alpha\boldsymbol{k}}(\boldsymbol{r},\sigma) = \varepsilon_{\alpha\boldsymbol{k}}\varphi_{\alpha\boldsymbol{k}}(\boldsymbol{r},\sigma)$$

Chamel (2012): $B(\boldsymbol{r})$ and $U(\boldsymbol{r})$ from energy minimisation

Watanabe& Pethick (2017): $B(r) \equiv \hbar^2/(2m_n)$ and $U(r) = 2V_K \cos(Kr)$

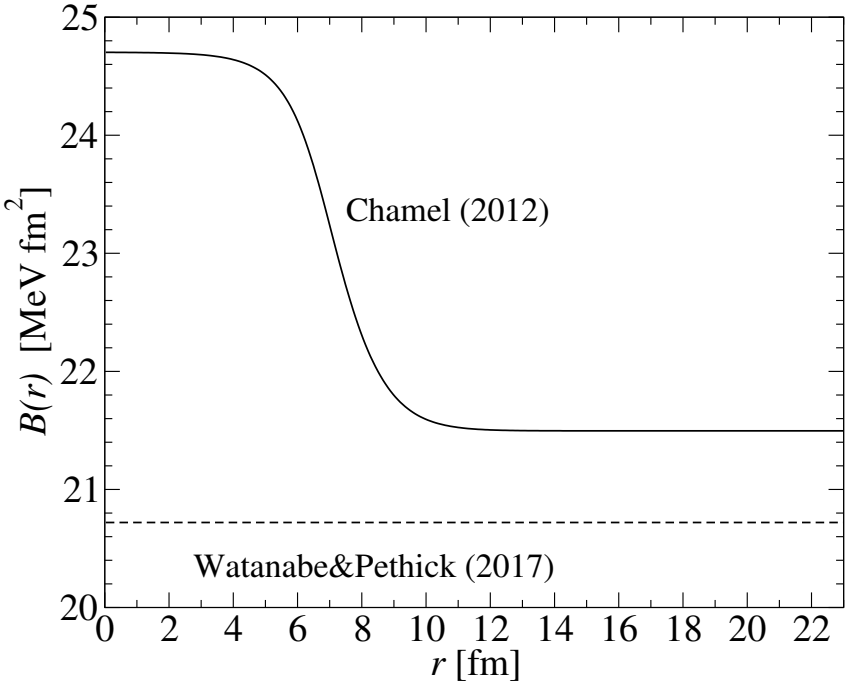

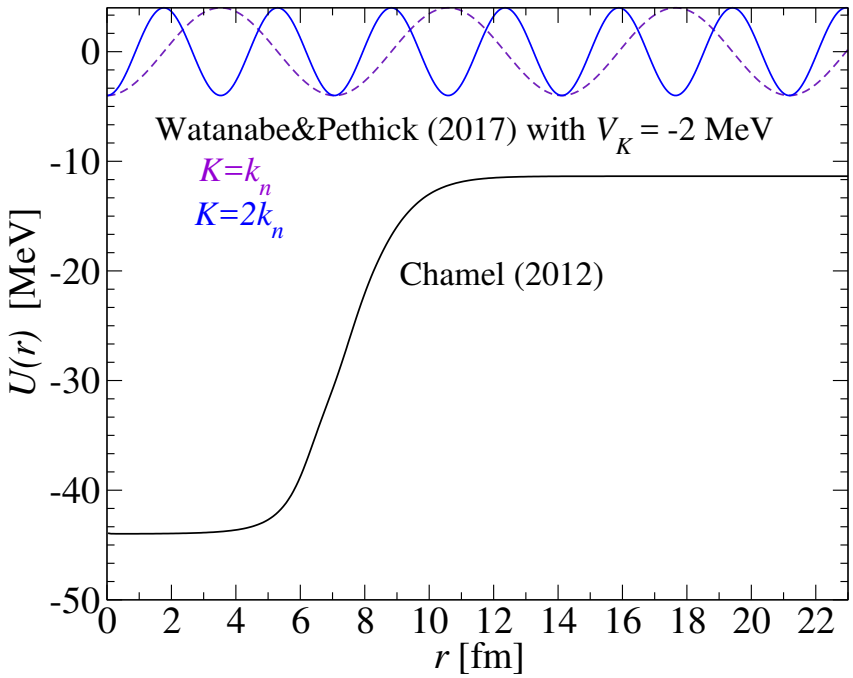

Watanabe&Pethick considered **unrealistically weak potentials**.

Role of pairing further examined

- full **3D band-structure** calculations (body-centered cubic lattice)
- same potentials $B(\boldsymbol{r})$ and $U(\boldsymbol{r})$ as those employed in 2012
- pairing included in the **BCS approximation**
- analytical formula

$$n_n^s = \frac{m_n}{24\pi^3\hbar^2}\sum_\alpha \int |\nabla_{\boldsymbol{k}}\varepsilon_{\alpha\boldsymbol{k}}|^2 \frac{\Delta^3}{\sqrt{(\varepsilon_{\alpha\boldsymbol{k}}-\mu)^2+\Delta^2}^3}\mathrm{d}^3k$$

- **whole range of gaps** up to largest possible values:

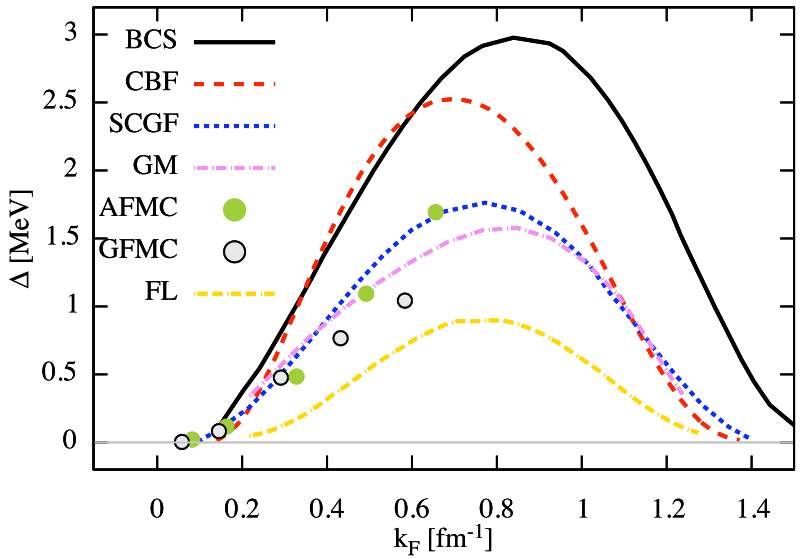

Adapted from Sedrakian&Clark, arXiv:1802.00017

Role of pairing further examined

Numerical results obtained using a new parallelized code based on plane waves using FFT and solid-state numerical techniques.

Δ (MeV)	$\Delta/\varepsilon_{\mathrm{F}}$	n_n^s/n_n^f (%)
3.09	0.169	7.85
2.15	0.117	7.72
1.49	0.0813	7.61
1.04	0.0567	7.55
0.721	0.0393	7.53
0.501	0.0273	7.56
0.348	0.0190	7.61
0.242	0.0132	7.67
0.168	0.00917	7.73
0.117	0.00638	7.78
0	0	7.84

$27 \times 27 \times 27$ FFT points ($\delta r \sim 0.9$ fm)

1650 bands (half without pairing)

BZ integrations with 65280 $\boldsymbol{k}$ points.

extensive convergence tests

Chamel, in prep.

Validity of weak coupling approximation confirmed.

Including pairing is computationally very costly, but results are essentially the same as those obtained without.

Role of quantum zero point motion and pairing

Kobyakov&Pethick speculated that band-structure effects could be suppressed by quantum zero-point motion of ions.

Phys. Rev. C 87, 055803 (2013)

Δ (MeV)	n_n^s/n_n^f (%)
3.09	8.21
2.15	8.04
1.49	7.92
1.04	7.86
0.721	7.85
0.501	7.88
0.348	7.92
0.242	7.97
0.168	8.02
0.117	8.06
0	8.10

$B(\boldsymbol{r})$ and $U(\boldsymbol{r})$ modified by Debye-Waller factor using bare ion mass M.

In reality, zero-point motion damped ($M^* \gg M$).

Chamel, in prep.

Superfluid fraction only slightly increased, but overestimate.

All in all, superfluid neutrons are still strongly entrained by the crust.

Superfluid reservoir and giant pulsar glitches

The superfluid in the crust does not carry enough angular momentum!
Andersson et al., PRL 109, 241103; Chamel, PRL 110, 011101 (2013)

We have calculated $I_{\rm crust}/I$ considering *unified* equations of state based on accurately calibrated nuclear models:

The inferred mass of Vela is at most $0.66 M_\odot$, corresponding to central densities $\bar{n} \approx 0.23 - 0.33$ fm^{-3}.

At such densities, the equation of state is fairly well constrained by laboratory experiments.

Delsate et al., Phys.Rev.D94, 023008(2016)

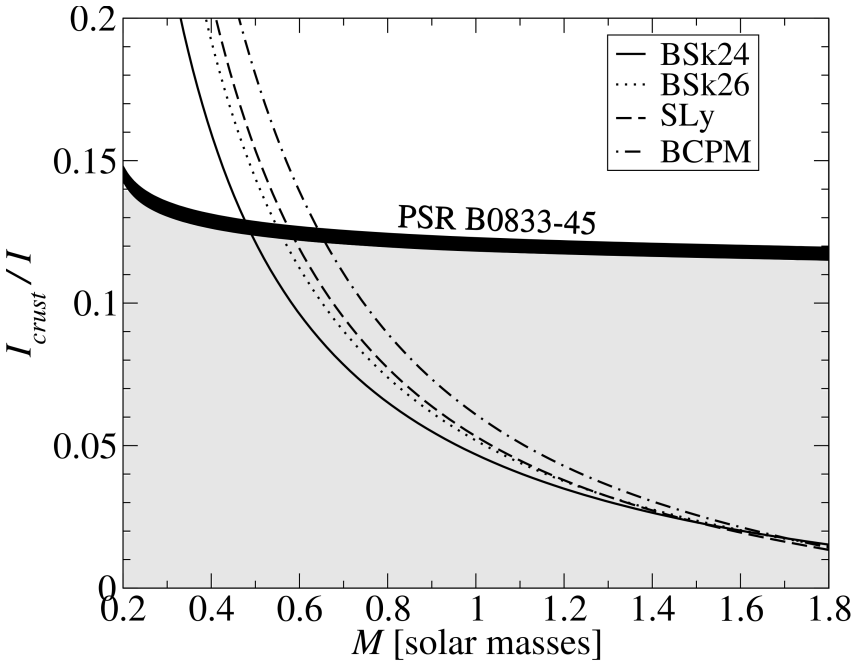

This conclusion has been confirmed by other groups.

Entrainment and collective excitations

Entrainment impacts low-energy collective excitations:

- clusters are effectively heavier $M^* > M$,
- lattice and superfluid longitudinal excitations are mixed.

Chamel,Page,Reddy,Phys.Rev.C87,035803(2013)

Chamel,Page,Reddy,J.Phys. Conf.Ser.665, 012065 (2016).

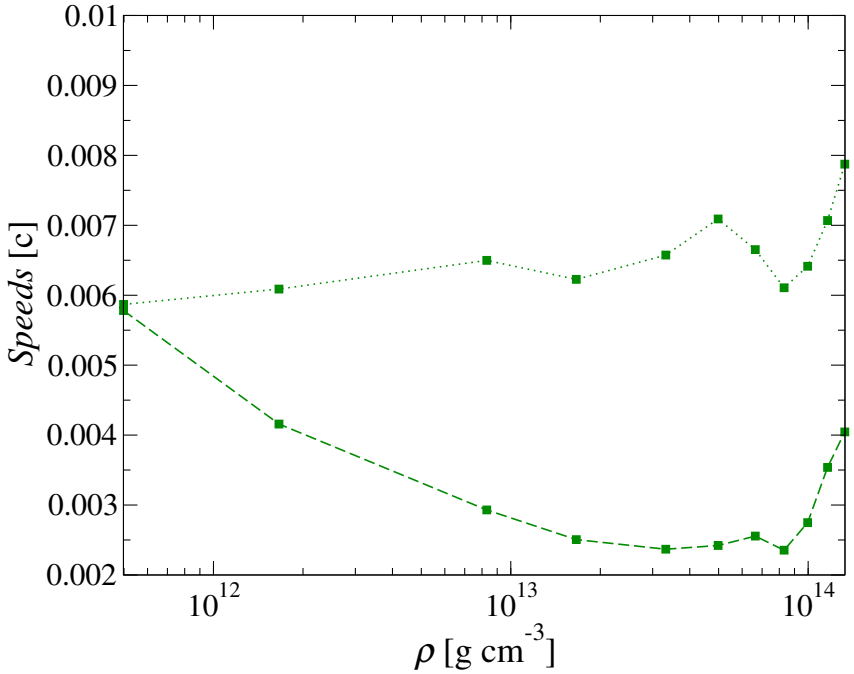

Transverse lattice phonon speeds with (dashed line) and without (dotted line) entrainment.

Entrainment and collective excitations

Entrainment impacts low-energy collective excitations:

- clusters are effectively heavier $M^* > M$,
- lattice and superfluid longitudinal excitations are mixed.

Chamel,Page,Reddy,Phys.Rev.C87,035803(2013)

Chamel,Page,Reddy,J.Phys. Conf.Ser.665, 012065 (2016).

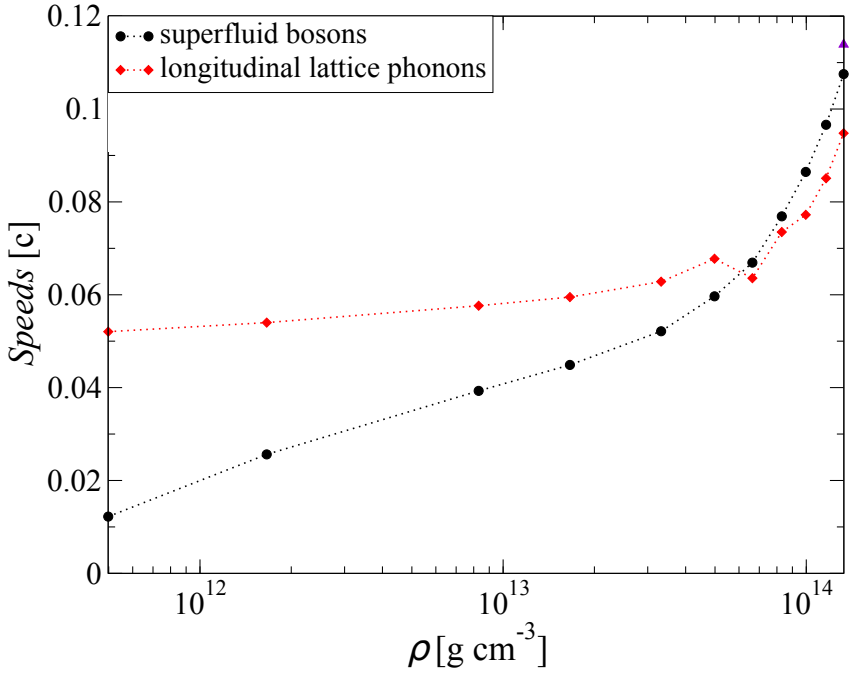

No entrainment, no mixing

Entrainment and collective excitations

Entrainment impacts low-energy collective excitations:

- clusters are effectively heavier $M^* > M$,
- lattice and superfluid longitudinal excitations are mixed.

Chamel,Page,Reddy,Phys.Rev.C87,035803(2013)

Chamel,Page,Reddy,J.Phys. Conf.Ser.665, 012065 (2016).

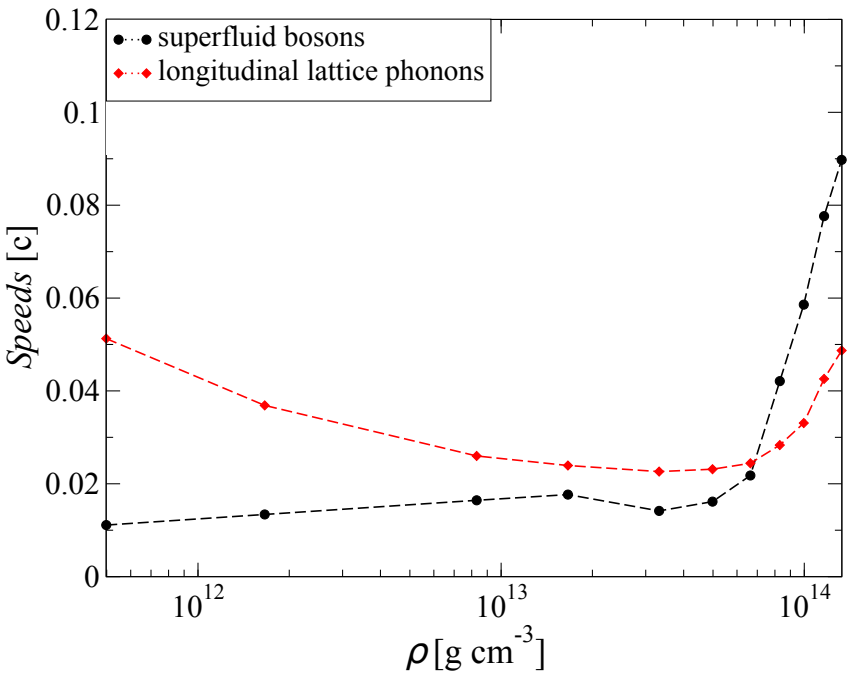

Entrainment, no mixing

Entrainment and collective excitations

Entrainment impacts low-energy collective excitations:

- clusters are effectively heavier $M^* > M$,
- lattice and superfluid longitudinal excitations are mixed.

Chamel,Page,Reddy,Phys.Rev.C87,035803(2013)

Chamel,Page,Reddy,J.Phys. Conf.Ser.665, 012065 (2016).

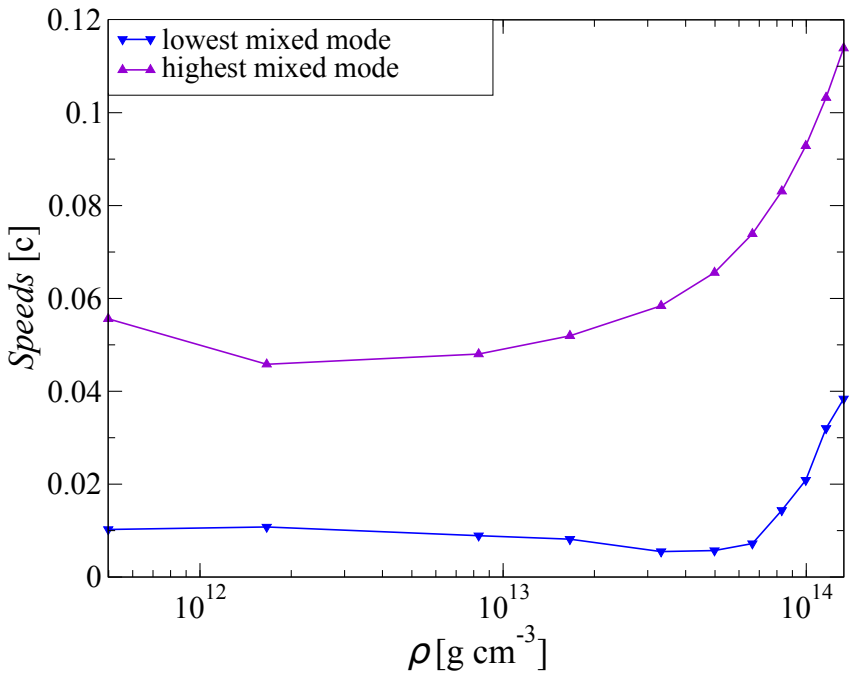

Entrainment and mixing

Entrainment and thermal properties

The contribution of collective excitations to the specific heat at low T varies like $(k_B T/\hbar v)^3$. Since entrainment reduces the speed v of the phonon modes, the specific heat is enhanced.
Chamel,Page,Reddy,Phys.Rev.C87,035803(2013)
Chamel,Page,Reddy,J.Phys. Conf.Ser.665, 012065 (2016).

Contributions to the crustal specific heat at $T = 10^7$ K :

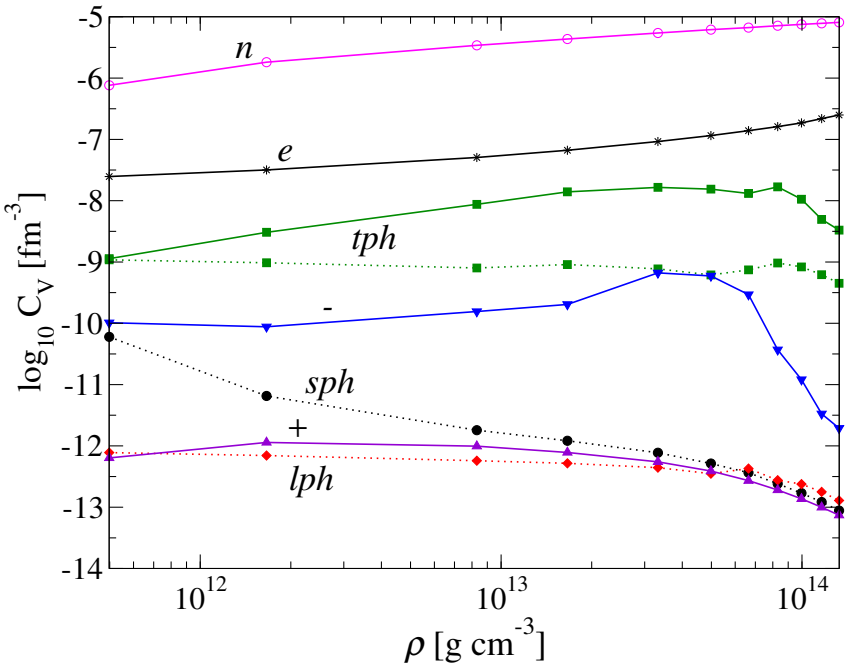

n normal neutrons
e electrons
tph transverse lattice phonons
lph longitudinal lattice phonons (without mixing)
sph superfluid phonons (without mixing)
$\pm$ longitudinal mixed modes

Entrainment and thermal properties

The contribution of collective excitations to the specific heat at low T varies like $(k_B T/\hbar v)^3$. Since entrainment reduces the speed v of the phonon modes, the specific heat is enhanced.
Chamel,Page,Reddy,Phys.Rev.C87,035803(2013)
Chamel,Page,Reddy,J.Phys. Conf.Ser.665, 012065 (2016).

Contributions to the crustal specific heat at $T = 10^8$ K :

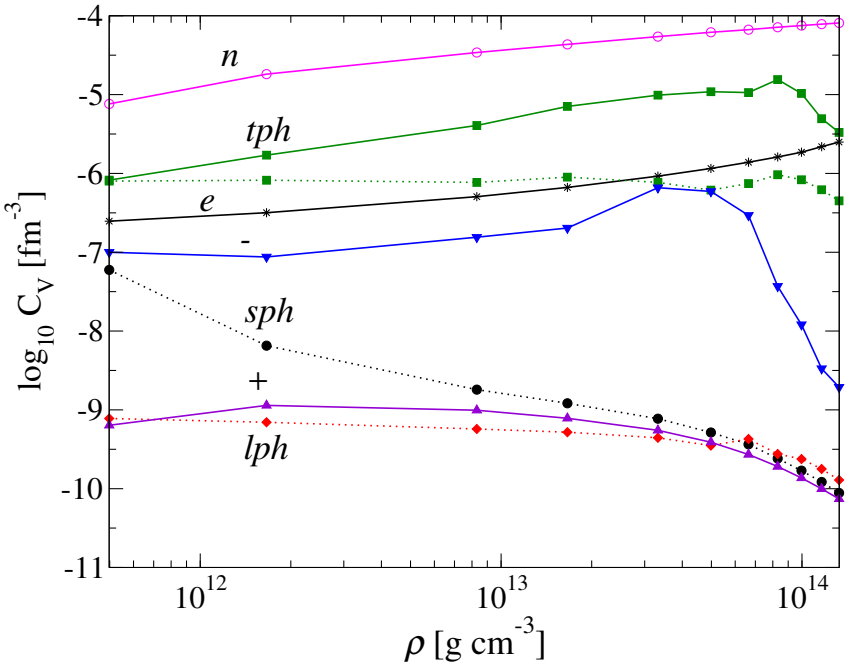

n normal neutrons
e electrons
tph transverse lattice phonons
lph longitudinal lattice phonons (without mixing)
sph superfluid phonons (without mixing)
$\pm$ longitudinal mixed modes

Entrainment and thermal properties

The contribution of collective excitations to the specific heat at low T varies like $(k_B T/\hbar v)^3$. Since entrainment reduces the speed v of the phonon modes, the specific heat is enhanced.
Chamel,Page,Reddy,Phys.Rev.C87,035803(2013)
Chamel,Page,Reddy,J.Phys. Conf.Ser.665, 012065 (2016).

Contributions to the crustal specific heat at $T = 10^9$ K :

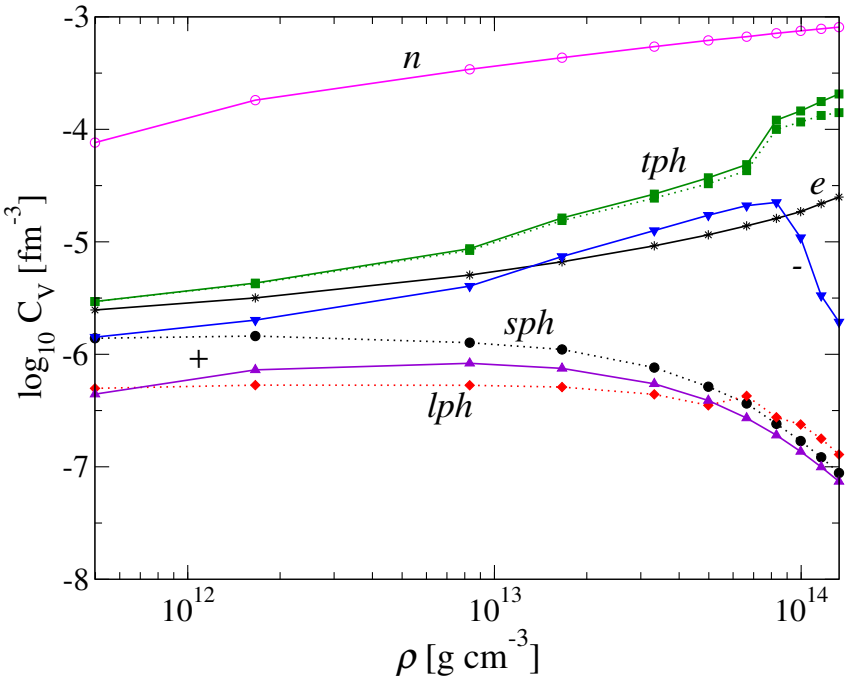

n normal neutrons
e electrons
tph transverse lattice phonons
lph longitudinal lattice phonons (without mixing)
sph superfluid phonons (without mixing)
$\pm$ longitudinal mixed modes

Entrainment and thermal properties

Changes in phonon velocities impact the electron-phonon scattering hence also the (electron) thermal conductivity.

All in all, entrainment leads to an increase of the thermal relaxation time of the crust.

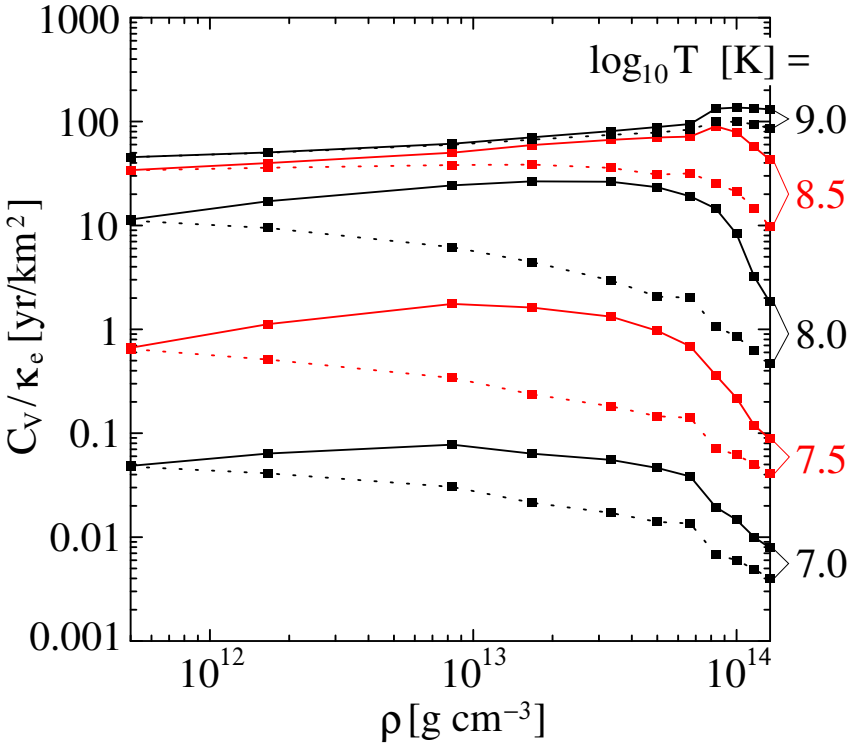

Thermal properties were calculated for catalyzed crusts; they may be different for accreted crusts.

Chamel et al.,Phys.Rev.C87,035803(2013)

Conclusions

What we have learned:

- **Superfluid neutrons in neutron-star crusts do not flow freely** due to the breaking of translational symmetry.
- **3D band-structure calculations including pairing and lattice vibrations** confirm the suppression of superfluidity.
- The strong depletion of the crustal superfluid reservoir has **implications for the interpretation of giant pulsar glitches**.
- Entrainment **impacts transport properties and the cooling of neutron stars**.

Open questions:

- Role of the spatial arrangement of clusters (disorder)?
- Role of the composition (accreted vs catalyzed crusts)?
- Role of a strong magnetic field?